

Study of Deformed Odd- A Nuclei by the (d,p) Reaction*

MICHEL N. VERGNES† AND RAYMOND K. SHELIN

Florida State University, Tallahassee, Florida

(Received 3 June 1963)

Yb^{176} (97.5%) and Hf^{178} (95.5%) targets have been bombarded with 12-MeV deuterons. The protons emerging from the (d,p) reaction were analyzed with ≈ 15 -keV energy resolution at many angles utilizing a single gap, broad range magnetic spectrograph. Up to 3 MeV, 55 states have been observed in Yb^{177} and 60 in Hf^{179} . Most of these states were previously unknown. The lowest energy levels in both Yb^{177} and Hf^{179} can definitely be identified with the intrinsic Nilsson orbitals $\frac{5}{2}^+$ (624), $\frac{3}{2}^-$ (514), and $\frac{1}{2}^-$ (510) and their associated rotational bands. The absolute cross sections and the angular distributions of the protons were measured for the reaction $\text{Yb}^{176}(d,p)\text{Yb}^{177}$. The experimental results agree very well with the predictions of the Satchler and Tobocman stripping theory for deformed nuclei. It is, therefore, established that this theory can furnish a valuable criterion for assigning spins and Nilsson orbitals in deformed nuclei. The discrepancy between experimental and calculated values of the decoupling parameter, a , for the $\frac{1}{2}^-$ (510) band can be resolved if one replaces, in the expansion of the wave function, the theoretical Nilsson coefficients by experimentally determined coefficients. This seems to indicate that (d,p) reactions may be a useful aid in determining detailed properties of the wave functions for deformed nuclei. A comparison of the lowest states of the 107 neutron isotones Yb^{177} , Hf^{179} , W^{181} , and Os^{183} is presented.

I. INTRODUCTION

IT has recently been shown¹⁻⁶ that (d,p) stripping reactions can be used to study the excited levels of spherical nuclei near the neutron closed shells $N=82$ and $N=126$. The comparisons with theory clearly indicate that the spherical shell model, corrected when necessary to take into account pairing interactions, gives an adequate description of these nuclei. In the intermediate region between two closed shells, the nuclei possess a permanent ellipsoidal deformation and the spherical shell model no longer applies. The collective properties of these nuclei are well described by the unified model.⁷ Using this model, the distorted-wave Born approximation and, for intrinsic excitations, the Nilsson wave functions,⁸ it is possible⁹ to compute the theoretical differential cross section for the capture of a neutron by the (d,p) reaction into any Nilsson orbital or rotational state built upon one of these orbitals.

Very few attempts¹⁰⁻¹² have been made until recently

to test or to use these results and none of them can be considered completely satisfactory.

The principal purpose of the work reported in this paper is to test the validity of the theory for the capture of a neutron by the (d,p) reaction into excited levels of a deformed odd- A nucleus in the rare-earth region. The nucleus Yb^{177} with 107 neutrons was used for this test. Excited levels of Hf^{179} were also studied by the (d,p) reaction and compared to the levels of Yb^{177} and other 107-neutron isotones.

II. THEORETICAL CALCULATIONS

The differential cross section for a (d,p) stripping reaction on an even-even target nucleus may be written in a simple form¹³

$$d\sigma_{l,\alpha}(\theta)/d\omega = (2I+1)S_l\phi_l(\theta), \quad (1)$$

where I is the angular momentum and α represents the other quantum numbers of the residual nucleus; l is the orbital angular momentum of the captured neutron. The spectroscopic factor S_l contains all the information about nuclear structure and $\phi_l(\theta)$, the intrinsic single-particle cross section, contains all the angular dependence of the cross section. This intrinsic single-particle cross section can be computed using the simple Butler theory¹⁴ or the more sophisticated distorted-wave Born approximation (DWBA) of Tobocman.¹⁵ The authors are extremely indebted to G. R. Satchler who performed this computation for the reaction $\text{Yb}^{176}(d,p)\text{Yb}^{177}$, at an incident deuteron energy of 12 MeV and for Q values of 1, 2, and 3 MeV, using the Tobocman theory and appropriate optical potentials and cutoff radii.

Using for the target and residual nuclei the unified model wave functions and for the intrinsic excitations the Nilsson wave functions, Satchler⁹ has obtained an

* Work supported in part by the U. S. Atomic Energy Commission.

† On leave from Institut du Radium, Laboratoire Joliot Curie de Physique Nucléaire, Orsay, France.

¹ R. H. Stokes, Phys. Rev. **121**, 613 (1961).

² G. B. Holm and H. J. Martin, Phys. Rev. **122**, 1537 (1961).

³ D. W. Miller, H. E. Wegner, and W. S. Hall, Phys. Rev. **125**, 2054 (1962).

⁴ J. R. Erskine, W. W. Buchner, and H. A. Enge, Phys. Rev. **128**, 720 (1962).

⁵ R. H. Fulmer, A. L. McCarthy, and B. L. Cohen, Phys. Rev. **128**, 1302 (1962).

⁶ F. W. Bingham and M. B. Sampson, Phys. Rev. **128**, 1796 (1962).

⁷ A. Bohr and B. R. Mottelson, Kgl. Danske Videnskab. Selskab, Mat. Fys. Medd. **27**, No. 16 (1953).

⁸ S. G. Nilsson, Kgl. Danske Videnskab. Selskab, Mat. Fys. Medd. **29**, No. 16 (1955).

⁹ G. R. Satchler, Ann. Phys. (N. Y.) **3**, 275 (1958).

¹⁰ G. B. Holm, G. R. Burwell, and D. W. Miller, Phys. Rev. **122**, 1260 (1961).

¹¹ R. A. Harlan, thesis, Florida State University, Tallahassee, 1963 (unpublished).

¹² Akira Isoya, Phys. Rev. **130**, 234 (1963).

¹³ J. B. French and B. J. Raz, Phys. Rev. **104**, 1411 (1956).

¹⁴ S. T. Butler, Proc. Roy. Soc. (London) **A208**, 559 (1951).

¹⁵ W. Tobocman, Phys. Rev. **115**, 99 (1959).

expression for the spectroscopic factor for a deformed nucleus

$$S_I(I, \Omega, N) = [2/(2I+1)] C_{I, I}^2(\Omega, N), \quad (2)$$

where N is the principal quantum number of the Nilsson oscillator and Ω is equal to the projection of I on the nuclear axis. The $C_{j, I}(\Omega, N)$ are normalized coefficients of the expansion of the Nilsson wave function $\chi(\Omega, N)$ as a series of wave functions of definite j :

$$\chi(\Omega, N) = \sum_{j, I} C_{j, I}(\Omega, N) \varphi_{j, I}(\Omega, N), \quad (3)$$

where

$$\sum_{j, I} C_{j, I}^2(\Omega, N) = 1. \quad (3')$$

In formula (2), the coefficient is labeled $C_{I, I}(\Omega, N)$ because for an even-even target nucleus j has to be equal to the angular momentum I .

The coefficients $C_{j, I}(\Omega, N)$ are related to the Nilsson coefficients⁸ $a_{I, \Lambda}(\Omega, N)$ by a Clebsch-Gordan transformation:

$$C_{j, I}(\Omega, N) = \sum_{\Lambda} a_{I, \Lambda}(\Omega, N) \langle I, \frac{1}{2}, \Lambda, \Sigma | I, \Omega \rangle. \quad (4)$$

The table of these coefficients $C_{j, I}(\Omega, N)$ for all the neutron Nilsson orbitals to be expected in rare-earth deformed nuclei is given in the Appendix.

The theoretical differential cross section for a (*d, p*) reaction on an even-even target nucleus, leaving the residual nucleus in a state of angular momentum I with Nilsson quantum numbers Ω and N , can then be written as

$$d\sigma_{I, I, \Omega, N}(\theta)/d\omega = 2C_{I, I}^2(\Omega, N) \phi_I(\theta). \quad (5)$$

III. EXPERIMENTAL PROCEDURES

A 12-MeV deuteron beam of the Florida State University Tandem Van de Graaff accelerator¹⁶ was used to produce the (*d, p*) reactions. The beam intensity in the reaction chamber was approximately 0.25 μ A, varying from a minimum value of 0.15 μ A to a maximum value of 0.65 μ A. The total number of incoming deuterons was measured by using a Faraday cup and an integrator. The precision of this measurement was of the order of 1 to 2% for the long runs involved.

The protons emerging after (*d, p*) reaction were analyzed with a single-gap, broad-range, magnetic spectrograph.¹⁷ The solid angle of this spectrograph is of the order of 0.7×10^{-4} sr for 15-MeV protons. Four Kodak nuclear emulsion plates positioned on the focal curve of the magnet are used as detectors. The angle θ between the magnet entrance slits and the direction of the incident beam can be varied between 0 and 132 deg.

Targets of isotopically enriched Yb¹⁷⁶ and Hf¹⁷⁸

oxides on thin carbon backings ($\approx 50 \mu\text{g}/\text{cm}^2$) were prepared by vacuum evaporation.^{11,18} The thickness at the center of one of the Yb targets was measured by Rutherford scattering as $\approx 0.7 \text{ mg}/\text{cm}^2$. The thicknesses of the other Yb and Hf targets were approximately the same. The targets were obviously not homogeneous. For this reason, in order to obtain the angular distribution of the protons after (*d, p*) reaction, it would have been necessary to measure the proton spectra at the different angles with the beam spot at exactly the same place on the target. Because of the long exposure times required, this was impossible.

Angular distributions were obtained, however, for the proton groups corresponding to excited levels of Yb¹⁷⁷ in the following way: Long exposures (6000 to 10 000 μ C) were taken at each of the following angles: 25°, 35°, 45°, 55°, 65°, 77°, 90°, 107°, and 125° at different times and with different positions of the beam on the target. These runs gave the relative intensities of the different proton groups at one angle with a good accuracy. Then, short exposures (2000 μ C) were taken in one long monitor run with a constant position of the beam on the target for all these angles. Comparison of the total number of proton tracks, in chosen regions of the plates, for the long exposure and the monitor exposure at a given angle, gave us a normalization of the long-exposure proton spectra. This normalization allowed the determination of the angular distributions of the different proton groups.

To obtain the absolute differential cross sections, it was necessary to know the value of the product of the thickness of the target times the solid angle of the spectrograph. This was measured during the monitor run by Rutherford scattering of 3.8-MeV deuterons on the target.

The systematic errors on the angular distributions resulting from the complicated procedure involved are believed not to be larger than 10 to 20%. The errors on the absolute cross sections are probably not bigger.

A program written¹⁷ for the IBM 709 was used to extract the Q values and the excitation energies from the proton spectra. The errors on the relative energies are generally less than 3 keV.

IV. Yb¹⁷⁶(*d, p*)Yb¹⁷⁷ REACTION

A typical proton spectrum for the reaction Yb¹⁷⁶(*d, p*)Yb¹⁷⁷ is shown in Fig. 1; the energy resolution (full width at half-maximum) is approximately 15 keV. The proton peaks corresponding to (*d, p*) reactions on light contaminants are easy to recognize and to eliminate because of their kinematic shift. The very high enrichment (97.5% of Yb¹⁷⁶) of the Yb oxide available and the fact that contamination by heavy nuclei during the preparation of the target is unlikely make it relatively certain that all but perhaps the smallest of the peaks left after elimination of the light impurities

¹⁶ The Tandem Van de Graaff program at Florida State University is supported in part by the U. S. Air Force Office of Scientific Research.

¹⁷ R. A. Kenefick, thesis, Florida State University, Tallahassee, 1962 (unpublished).

¹⁸ M. C. Olesen and B. Elbeck, Nucl. Phys. 15, 134 (1960).

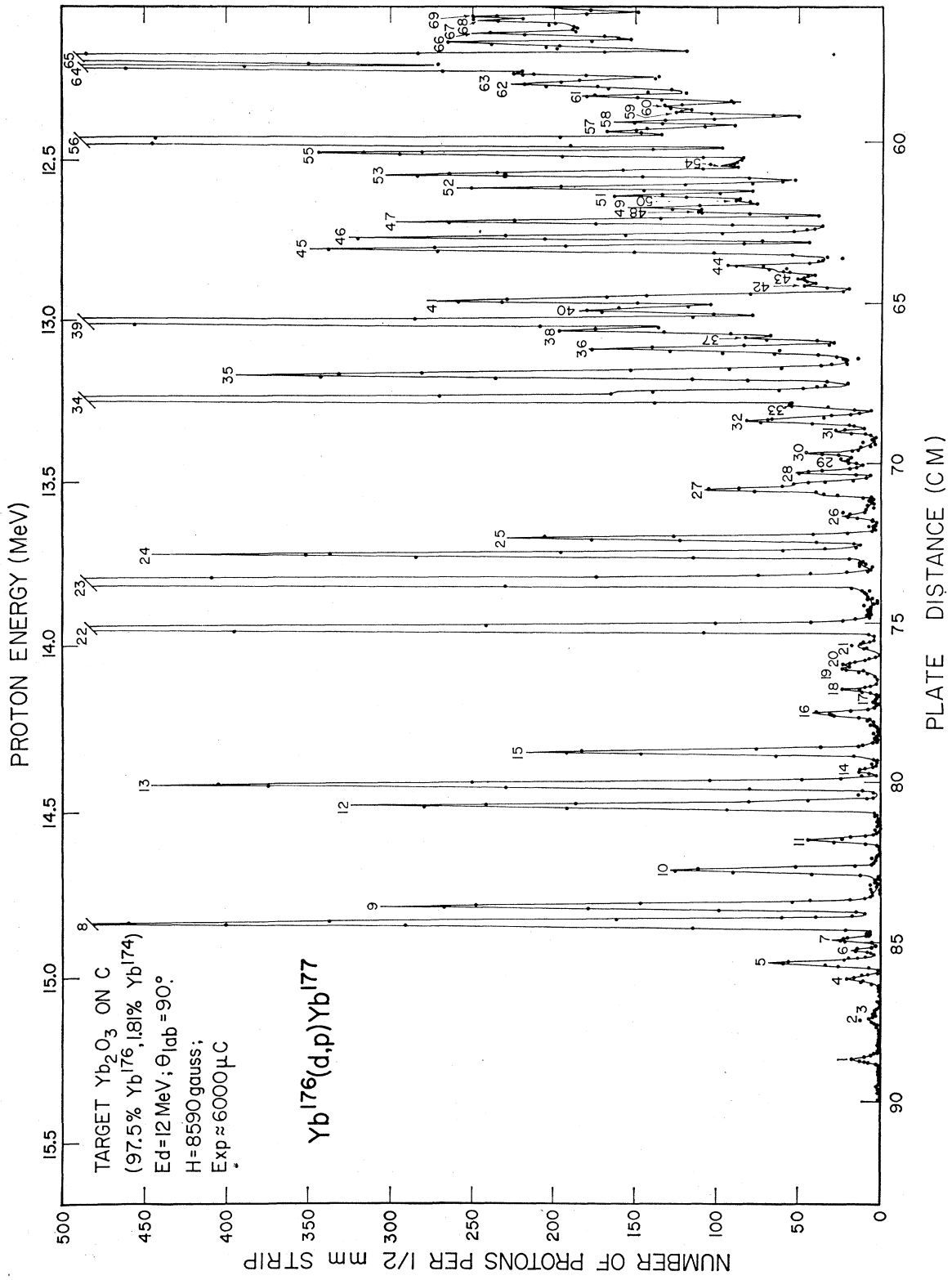
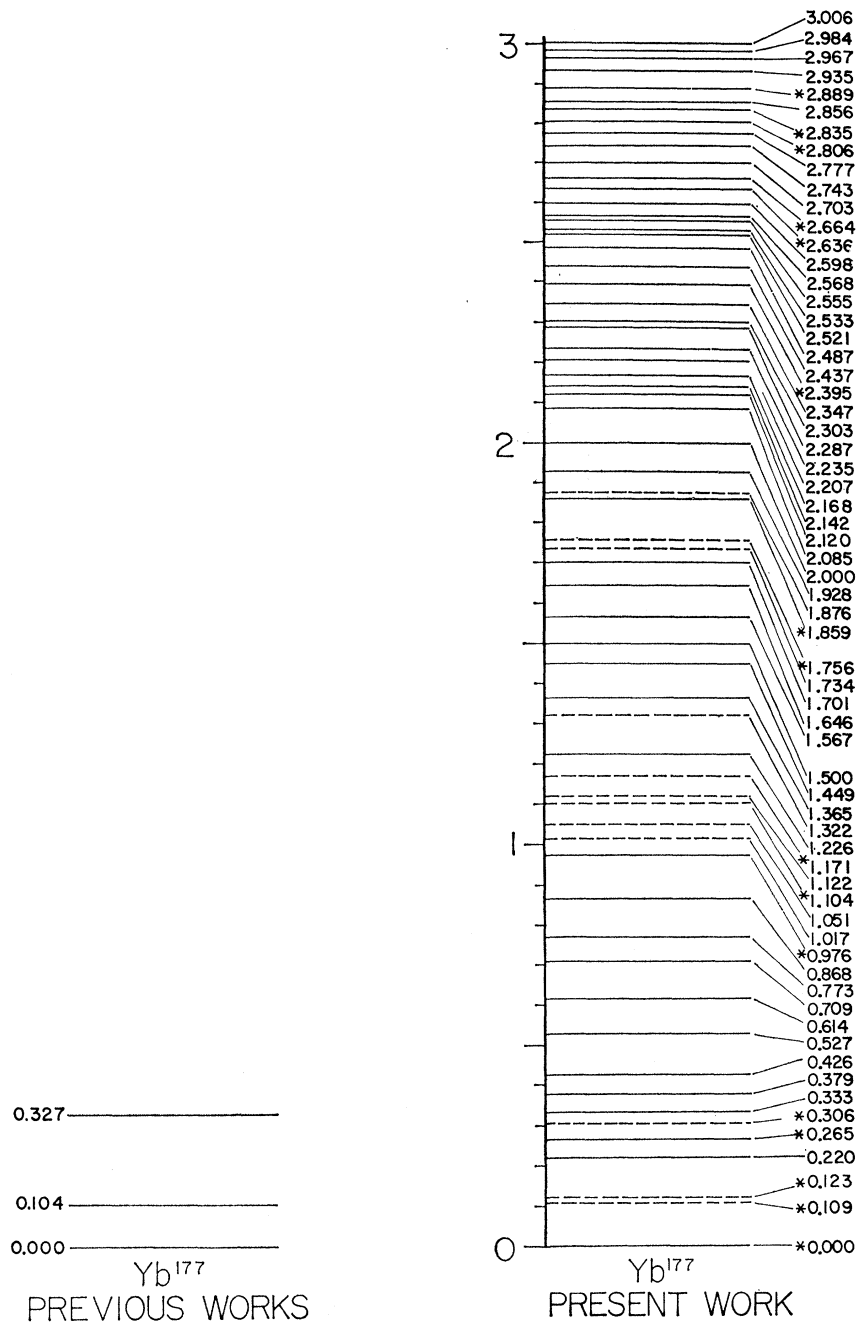


FIG. 1. Typical proton spectrum for the reaction $Yb^{176}(d,p)Yb^{177}$.

FIG. 2. Levels of Yb¹⁷⁷ up to an excitation energy of 3 MeV. The dashed levels correspond to very weak proton peaks in Fig. 1, which could possibly be due to other Yb isotopes or heavy impurities. The star indicates an uncertainty of more than 3 keV on the indicated energy.



can be assigned to the capture of a neutron into an excited state of Yb¹⁷⁷.

The levels obtained in this way by analysis of proton spectra taken at several angles are shown in Fig. 2, up to an excitation energy of 3 MeV. Table I gives the relative intensities of most of the proton peaks up to an excitation energy of 2.5 MeV; the normalization is such as to give at every angle an intensity of 1000 for the peak corresponding to the 379-keV excited level.

The mean experimental *Q* value for the ground-state

proton group is $Q=3340\pm 16$ keV, which is within error limits of the calculated¹⁹ value $Q=3277\pm 220$ keV.

A. Level Scheme

On the basis of the accurately determined energies of the excited states, it is easy to build a level scheme for Yb¹⁷⁷ up to an excitation energy of 700 keV including all but one of the levels found. The angular momentum,

¹⁹ L. A. Konig, J. H. E. Mattauch, and A. H. Wapstra, Nucl. Phys. 31, 1 (1962).

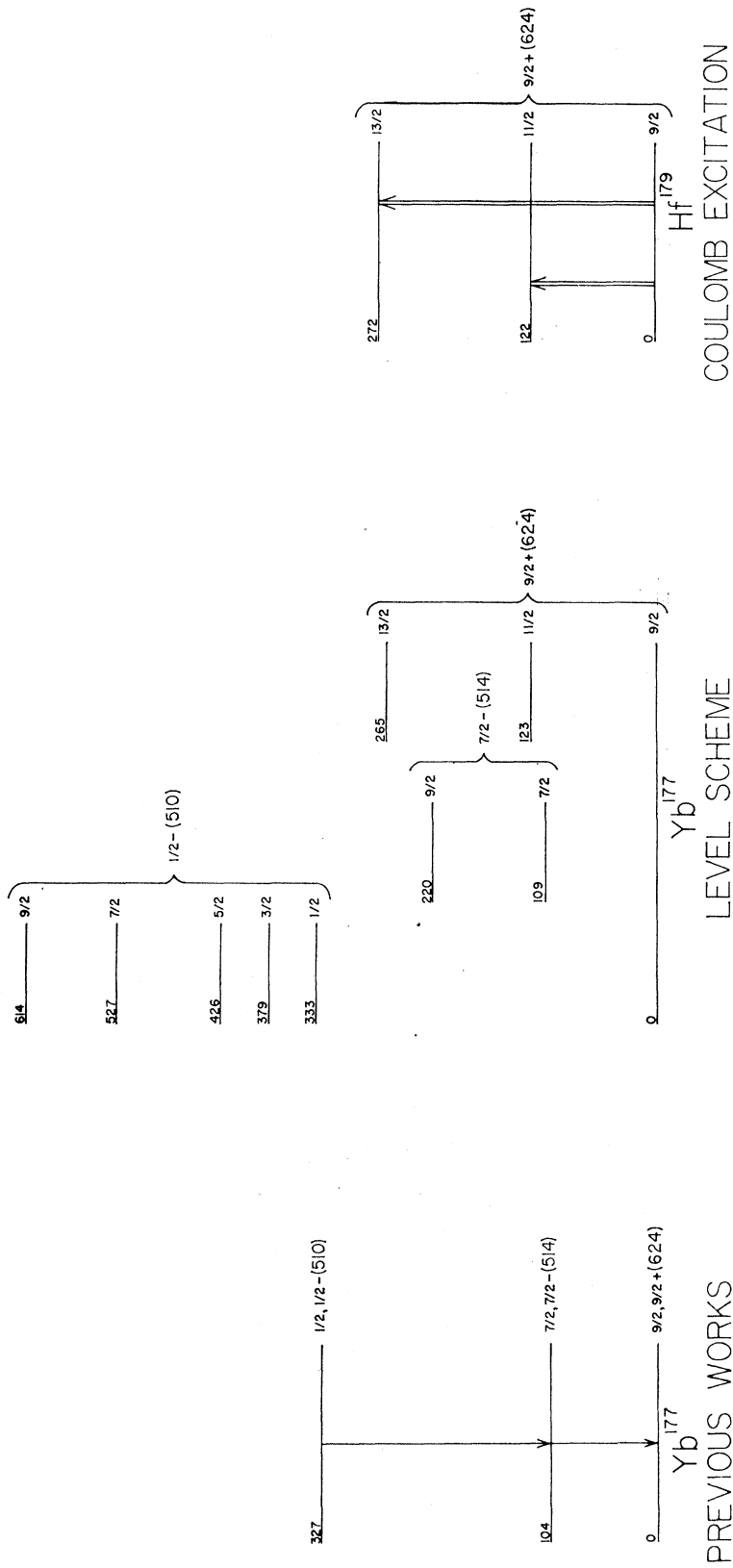


FIG. 3. Comparison of the level scheme obtained from (d, p) reaction data for the lowest excited states of Yb^{177} , with the level scheme previously known from the decay of the isomeric 327-keV level. The Coulomb excited levels of the isotope Hf^{179} are also indicated.

TABLE I. Relative intensities of the proton peaks for the $\text{Yb}^{176}(d, p)\text{Yb}^{177}$ reaction.^a

Excitation energy (keV)	Number of peak in Fig. 1	25°	35°	45°	55°	65°	77°	90°	107°
265	5	<i>a</i>	<i>w</i>	<i>w</i>	<i>w</i>	<i>w</i>	55	115	145
379	8	1000	1000	1000	1000	1000	1000	1000	1000
426	9	210	250	270	330	440	380	560	600
527	10	70	120	110	135	135	170	240	220
709	12	445	340	350	390	525	430	610	500
773	13	310	460	350	530	580	550	800	880
868	15	160	130	230	270	310	260	390	460
1226	22	440	<i>a</i>	670	775	960	>970	1500	1600
1365	23	1920	1990	1430	2580	2540	2650	3080	2790
1449	24	200	260	280	400	400	480	750	830
1500	25	310	320	<i>a</i>	280	320	230	410	420
1646	27	<i>a</i>	70	100	90	125	140	180	230
1859	32	<i>a</i>	<i>a</i>	55	<i>a</i>	100	100	>130	180
1928	34	1060	1120	920	1380	1060	1420	1890	~1700
2000	35	470	520	440	610	400	560	~800	~900
2085	36	170	130	<i>a</i>	225	200	200	330	390
2142	38	170	160	120	225	210	230	<330	<420
2168	39	760	980	760	1020	915	1080	1560	1530
2207	40	205	120	120	160	<i>a</i>	180	<300	<420
2235	41	170	170	185	250	<i>a</i>	300	450	580
2347	44	<i>w</i>	<i>w</i>	65	<i>a</i>	85	100	150	190
2395	45	225	300	320	410	290	470	>590	710
2437	46	320	300	290	400	380	390	610	640
2487	47	170	240	480	310	290	330	520	480

^a The entry "*a*" means that the peak is hidden at this angle by a light impurity peak; "*w*" indicates a weak peak (≤ 50).

parity, and Nilsson orbital were previously determined^{20,21} for the ground state and two excited states at 104 and 327 keV, which correspond to the 109- and 333-keV excited levels obtained by (d, p) reaction. The excited states at 123 and 265 keV correspond very well to the expected first two levels of the rotational ground-state band. This can be seen by a comparison with the results from Coulomb excitation^{22,23} of the isotone Hf^{179} . The excited state at 220 keV can be tentatively identified as the expected first rotational state of the $\frac{7}{2}^-$ (514) band. The 379-, 426-, 527-, and 614-keV levels can be fitted (see Table II) into an anomalous rotational band built upon the 333-keV $\frac{1}{2}^-$ (510) intrinsic level, with a decoupling parameter $a = +0.22$ and an inertial parameter $\hbar^2/2\mathcal{J} = 12.17$ keV. The 306-keV level not assigned corresponds probably to another Yb isotope.

In Fig. 3, the level scheme of Yb^{177} obtained from

 TABLE II. Energies of the rotational states of the $\frac{1}{2}^-$ (510) band.

$E_I - E_{1/2}$	I	$\frac{1}{2}$	$\frac{3}{2}$	$\frac{5}{2}$	$\frac{7}{2}$	$\frac{9}{2}$
Experimental	0	45.8 ± 1.7	93.3 ± 2.9	194.7 ± 4	281.5 ± 3.4	
Theoretical	0	44.54	92	195.94	281.37	

²⁰ K. W. Hoffman, I. Y. Krause, W. D. Schmid-Ott, and A. Flammersfeld, *Z. Physik* **160**, 201 (1960).

²¹ H. Morinaga and K. Takahashi, *Nucl. Phys.* **38**, 186 (1962).

²² N. P. Heydenburg and G. M. Temmer, *Phys. Rev.* **104**, 981 (1956).

²³ J. de Boer, M. Martin, and P. Marmier, *Helv. Phys. Acta* **32**, 377 (1959).

(d, p) reaction data is compared to previously known levels of Yb^{177} and to Coulomb excited levels of Hf^{179} .

B. Angular Distributions

The l values for the capture of a neutron into the lowest excited states of Yb^{177} can be determined by conservation of angular momentum and parity using the level scheme of Fig. 3. The DWBA curves corresponding to these predicted l values can then be compared to the experimental angular distributions. In this section, only the shapes of the distributions will be considered and no attention will be paid to the absolute values. These absolute values will be considered in the following section.

In Fig. 4, the shape of the experimental angular distribution of the protons corresponding to the 265-keV excited state is compared to the shape of the intrinsic

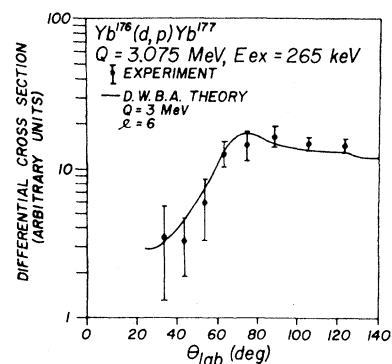


FIG. 4. Angular distributions for the 265-keV excited level in Yb^{177} .

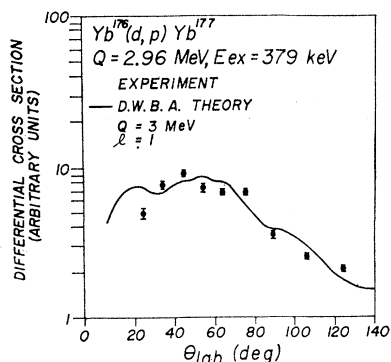


FIG. 5. Angular distributions for the 379-keV excited level in Yb^{177} .

single-particle cross section obtained using the distorted-wave Born approximation for the predicted value $l=6$. No other DWBA curve, corresponding to a different l value, could fit the experimental distribution. The errors indicated in Fig. 4 correspond only to the statistical errors. As was previously emphasized, large additional systematic errors (10–20%) are not unlikely.

In Fig. 5, the experimental distribution corresponding to the 379-keV excited level is compared to the predicted $l=1$ DWBA curve. In this case, the experimental distribution could also be fitted very well by the DWBA curve corresponding to $l=2$; values of $l=0$ or 3 cannot be completely excluded.

In Fig. 6, the experimental distributions corresponding to the 426- and 527-keV levels are compared to the predicted $l=3$ DWBA curve. This curve is the one which gives the best possible fit of the experimental distributions. However, values of $l=2$ or 4 can not be excluded.

The angular distribution corresponding to the 614-keV level can not be fitted by the predicted $l=5$ DWBA curve. No other DWBA curve except the one corresponding to $l=7$ can give a reasonable fit. The proton peak is probably a doublet, one member of which corresponds to the $\frac{9}{2}, \frac{1}{2}$ —(510) level.

These comparisons show that when the l values are known, there is a reasonably good agreement between the DWBA results and the experimental angular distributions. On the other hand, when the value of l

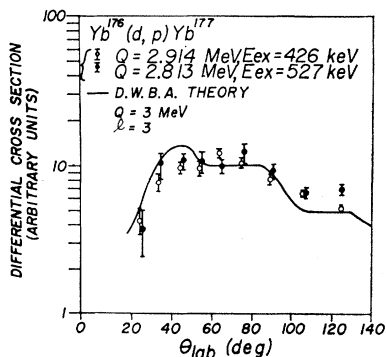


FIG. 6. Angular distributions for the 426- and 527-keV excited levels in Yb^{177} .

is not known, as is the case for the levels above 700 keV, such a comparison does not permit it to be determined uniquely. Because big systematic errors on the experimental results are possible and because the theoretical curves are not sensitive enough to the value of l , a reasonable fit can generally be obtained for three consecutive values of l .

The allowed l values obtained by this method for certain levels of Yb^{177} between 700 and 1500 keV are given in Table III. Only the levels corresponding to big proton peaks in Fig. 1 are included in this table. The statistical errors would make the comparison meaningless for the smallest peaks.

C. Differential Cross Sections

The theoretical differential cross sections for all the intrinsic Nilsson levels expected as excited states in a 107-neutron nucleus and their associated rotational bands were computed for $\theta=90^\circ$, using formula (5) and the coefficients $C_{l,l}$ given in the Appendix. The differ-

TABLE III. Analysis of some angular distributions in Yb^{177} .

Excitation energy	Peak number in Fig. 1	Allowed l values	Allowed I values
709	12	1(?), 2, 3	$\frac{1}{2}$ to $\frac{7}{2}$
773	13	2(?), 3	$\frac{3}{2}$ to $\frac{7}{2}$
868	15	3(?), 4	$\frac{5}{2}$ to $\frac{9}{2}$
976	16	4(?), 5(?), 7	$\frac{7}{2}$ to 15/2
1226	22	2, 3, 4(?)	$\frac{3}{2}$ to $\frac{9}{2}$
1365	23	0, 1, 2	$\frac{1}{2}$ to $\frac{5}{2}$
1449	24	2(?), 3(?)	$\frac{3}{2}$ to $\frac{7}{2}$
1500	25	0, 1, 2	$\frac{1}{2}$ to $\frac{5}{2}$

ential cross sections corresponding to the complete rotational band are given in the second column of Table IV. Rough estimates¹² of the factor U^2 which gives the probability that an orbital was not occupied in the target nucleus at the time of the reaction, are given in the third column of this table. Without pairing correlations, the factor U^2 would be equal to 0 for the “hole states,” and equal to 1.0 for the “particle states.” The effect of the pairing correlations on the cross sections can be roughly taken into account by multiplying the right side of expression (5) by the approximate factor U^2 ; the modified cross sections so obtained are indicated in the fourth column of Table IV.

In the level scheme of Fig. 3, definite Nilsson orbitals are assigned to the lowest levels of Yb^{177} . For these levels, therefore, it is possible to compare the theoretical differential cross sections with the corresponding absolute experimental differential cross sections. The good agreement observed in Fig. 7 shows that the expression of the spectroscopic factor obtained by Satchler is essentially right; it is also a good confirmation of our tentative level scheme. The fact that no normalization

was needed in order to obtain this agreement shows that the DWBA theory not only predicts correctly the variation with angle of the intrinsic single-particle cross section, as was shown in the preceding section, but also gives an absolute value in agreement with experiment.

D. Detailed Study of the $\frac{1}{2}^-(510)$ Rotational Band

In Fig. 7, the experimental and theoretical cross sections are compared at a given angle. More detailed and precise results can be obtained if the experimental spectroscopic factors S_I are extracted from the measured cross sections using formula (1). This extraction was performed at nine different angles for the members of

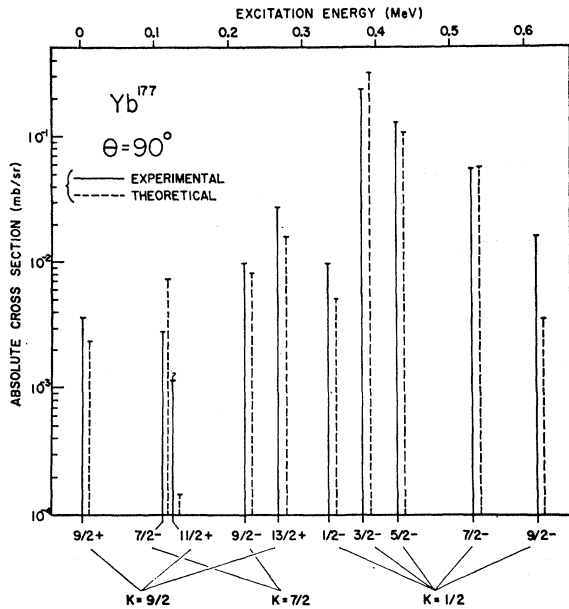


FIG. 7. Comparison of the experimental and theoretical absolute differential cross sections at an angle of 90° for the lowest excited levels of Yb^{177} . The pairing correlations were taken into account in computing the theoretical cross sections.

the rotational band $\frac{1}{2}^-(510)$ and, using formula (2), experimental coefficients $C_{I,l}^2$ were obtained whose mean values are compared to the square of the Nilsson coefficients in Table V.

A comparison of the sums of the squares of the experimental and theoretical coefficients up to $I=\frac{7}{2}$ shows clearly that no normalization of the experimental coefficients is needed.²⁴

$$\sum C_{I,l}^2(\text{Nilsson}) = 0.909; \quad \sum C_{I,l}^2(\text{exp}) = 0.915; \\ (\sigma = 0.041).$$

²⁴ In extracting the experimental coefficients $C_{I,l}^2$, a value of $U^2=1.0$ was assumed. If the value $U^2=0.91$ of Table IV were used, a normalization factor could prove necessary, but it would not be very different from 1.0.

TABLE IV. Total theoretical differential cross section at $\theta=90^\circ$.

Intrinsic level	$(d\sigma/d\omega)$ (mb/sr)	U^2	$U^2(d\sigma/d\omega)$ (mb/sr)
$\frac{1}{2}^-(521)^a$	0.47	$<0.1^b$	<0.047
$\frac{7}{2}^+(633)^a$	0.0368	$<0.1^b$	<0.037
$\frac{5}{2}^-(512)^a$	0.334	0.12	0.04
$\frac{7}{2}^-(514)^a$	0.0596	$\sim 0.4^b$	~ 0.024
$\frac{9}{2}^+(624)$	0.027	0.67	0.018
$\frac{3}{2}^-(510)$	0.484	0.91	0.44
$\frac{3}{2}^-(512)$	0.402	0.96	0.386
$\frac{7}{2}^-(503)$	0.381	1	0.38
$11/2^+(615)$	0.026	1	0.026
$\frac{9}{2}^-(505)$	0.051	1	0.051
$13/2^+(606)$	0.026	1	0.026
$\frac{3}{2}^-(501)$	0.966	1	0.966
$\frac{5}{2}^-(503)$	0.46	1	0.46
$\frac{1}{2}^-(501)$	0.98	1	0.98

^a Hole state.

^b Interpolated or extrapolated values.

The sums have practically the same value, close to 1.0, which should be the value of the sum for the complete rotational band.

Although of the same order of magnitude, the experimental coefficients are clearly different from the Nilsson coefficients. Accordingly, it is reasonable to wonder if these experimentally determined coefficients could give a better description of the deformed nucleus Yb^{177} in its excited state $\frac{1}{2}^-(510)$ than the Nilsson coefficients. If no final answer can be given here to this question, at least a simple test can be made. The decoupling parameter of the $\frac{1}{2}^-$ band is a function of the coefficients $C_{I,l}$:

$$a = \sum_j (-1)^{j-1/2} (j + \frac{1}{2}) C_{j,l}^2.$$

The values obtained using this formula can be compared to the experimental value, $a = +0.22$, obtained from the energies of the levels. With the Nilsson coefficients, the right order of magnitude is obtained, but the wrong sign: $a = -0.25$. Replacing the Nilsson coefficients by the experimental coefficients up to $I=\frac{7}{2}$, a good agreement is obtained: $a = +0.226$; ($\sigma=0.1$). The error is large but the agreement observed is at least encouraging.

TABLE V. Comparison of experimental and theoretical $C_{I,l}^2$ coefficients for the $\frac{1}{2}^-(510)$ rotational band in Yb^{177} .

I	l	$C_{I,l}^2(\text{Nilsson})$	$C_{I,l}^2(\text{Experimental})$	$\sigma(\text{Standard error})$
1/2	1	0.067	0.017	0.0057
3/2	1	0.43	0.336	0.046
5/2	3	0.308	0.4	0.055
7/2	3	0.164	0.164	0.022
9/2	5	0.08	?	...
11/2	5	0.01	?	...

E. Excited Levels Above 700 keV

In view of the good agreement found for the excited levels up to 700 keV between the theory of stripping reactions in deformed nuclei and the experimental results, an attempt will be made in this section to use this theory to try to identify some of the excited levels above 700 keV.

The intrinsic Nilsson orbitals expected^{12,25} as excited levels in a 107-neutron nucleus and their total theoretical cross sections for $\theta=90^\circ$ are listed in Table IV.

The rotational band built upon the $\frac{3}{2}^-$ (512) intrinsic state is the first band with a large cross section to be expected above the $\frac{1}{2}^-$ (510) rotational band. The levels corresponding to the proton peaks 12, 13, 15, and 16 in Fig. 1 have the right relative energies to correspond to the first four levels of the $\frac{3}{2}^-$ (512) band, with an inertial parameter $\hbar^2/2g \approx 13$ keV. The l values predicted by the Nilsson model are, respectively, 1, 3, 3, and 5 for these four levels. Table III shows that these values are allowed by the angular distributions. The experimental differential cross sections for $\theta=90^\circ$ are compared to the theoretical values in Table VI.

Though the agreement is not very good for each separate member, the total experimental and theoretical cross sections are very similar. It will, therefore, be tentatively assumed that the intrinsic level $\frac{3}{2}^-$ (512) appears in Yb¹⁷⁷ at an energy of 709 keV.

The next expected rotational band having a large cross section is the $\frac{7}{2}^-$ (503) band. As can be seen in the Appendix, the coefficients $C_{l,1}$ are such that only the peak corresponding to the intrinsic level $\frac{7}{2}^-$, $\frac{7}{2}^-$ (503) should be visible in the proton spectrum. The theoretical cross section for this level at $\theta=90^\circ$ is 0.38 mb/sr, which agrees very well with the experimental cross section of 0.35 mb/sr for the 1226-keV level. From the cross section alone, this level could also be the $\frac{5}{2}^-$ (503) intrinsic state; as can be seen in Table III, the value $l=3$ predicted by the Nilsson model for the intrinsic orbitals $\frac{7}{2}^-$ (503) and $\frac{5}{2}^-$ (503) is allowed for the 1226 keV. The proton peak corresponding to the 1226-keV level (peak 22 in Fig. 1) is well separated from the following peak; for this reason the $\frac{5}{2}^-$ (503) assignment can be reasonably ruled out because the proton peak corresponding to the rotational level $\frac{7}{2}^-$, $\frac{5}{2}^-$ (503) should in this case appear between peaks 22 and 23. It will be tentatively assumed that the 1226-keV level corresponds to the $\frac{7}{2}^-$ (503) Nilsson orbital.

TABLE VI. $\frac{3}{2}^-$ (512) rotational band.

$\frac{I}{d\sigma/d\omega}$ (mb/sr)	$\frac{3}{2}$	$\frac{5}{2}$	$\frac{7}{2}$	$\frac{9}{2}$	$(d\sigma/d\omega)$ total
Theoretical	0.0822	0.25	0.0389	0.0064	0.378
Experimental	0.139	0.182	0.0895	0.018	0.428

²⁵ V. G. Solov'ev, Dokl. Akad. Nauk SSSR 133, 325 (1960) [translation: Soviet Phys.—Doklady 133, 325 (1960)].

TABLE VII. $\frac{3}{2}^-$ (501) rotational band.

$\frac{I}{d\sigma/d\omega}$ (mb/sr)	$\frac{3}{2}$	$\frac{5}{2}$	$\frac{7}{2}$	$(d\sigma/d\omega)$ total
Theoretical	0.862	0.0358	0.0155	0.913
Experimental	0.704	0.1714	0.0095	0.885

The $\frac{3}{2}^-$ (501) intrinsic level and its associated rotational band are the next set of states expected to exhibit a large cross section. The levels corresponding to peaks 23, 24, and 26 in Fig. 1 have the right relative energies to be the three first members of this band, with an inertial parameter $\hbar^2/2g \approx 16.6$ keV. The theoretical and experimental cross sections at $\theta=90^\circ$ are compared in Table VII. The agreement is satis-

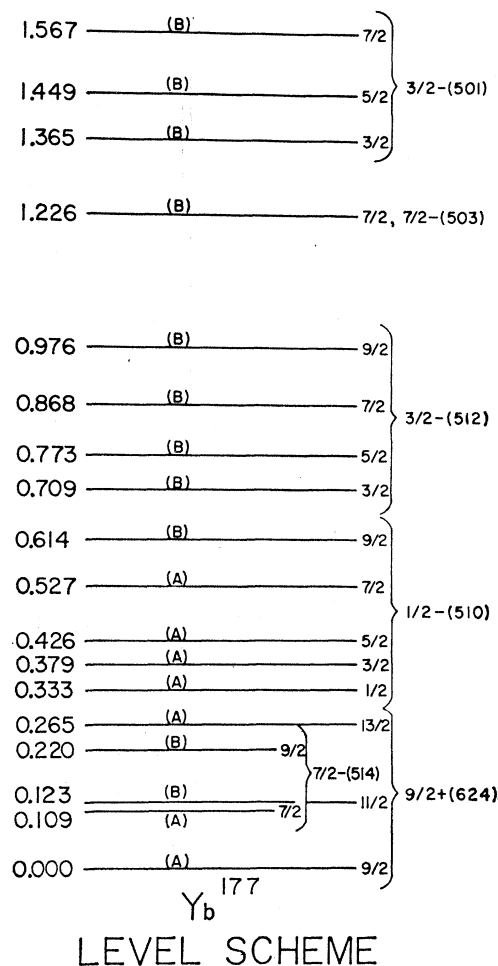


FIG. 8. Level scheme of Yb¹⁷⁷ up to an excitation energy of 1.6 MeV. Letter A means that the position of the level is sure and that the available data indicate quite strongly the angular momentum, parity, and Nilsson orbital. Letter B means that the position of the level is well established, but that angular momentum, parity, and Nilsson orbital indicated are only tentative.

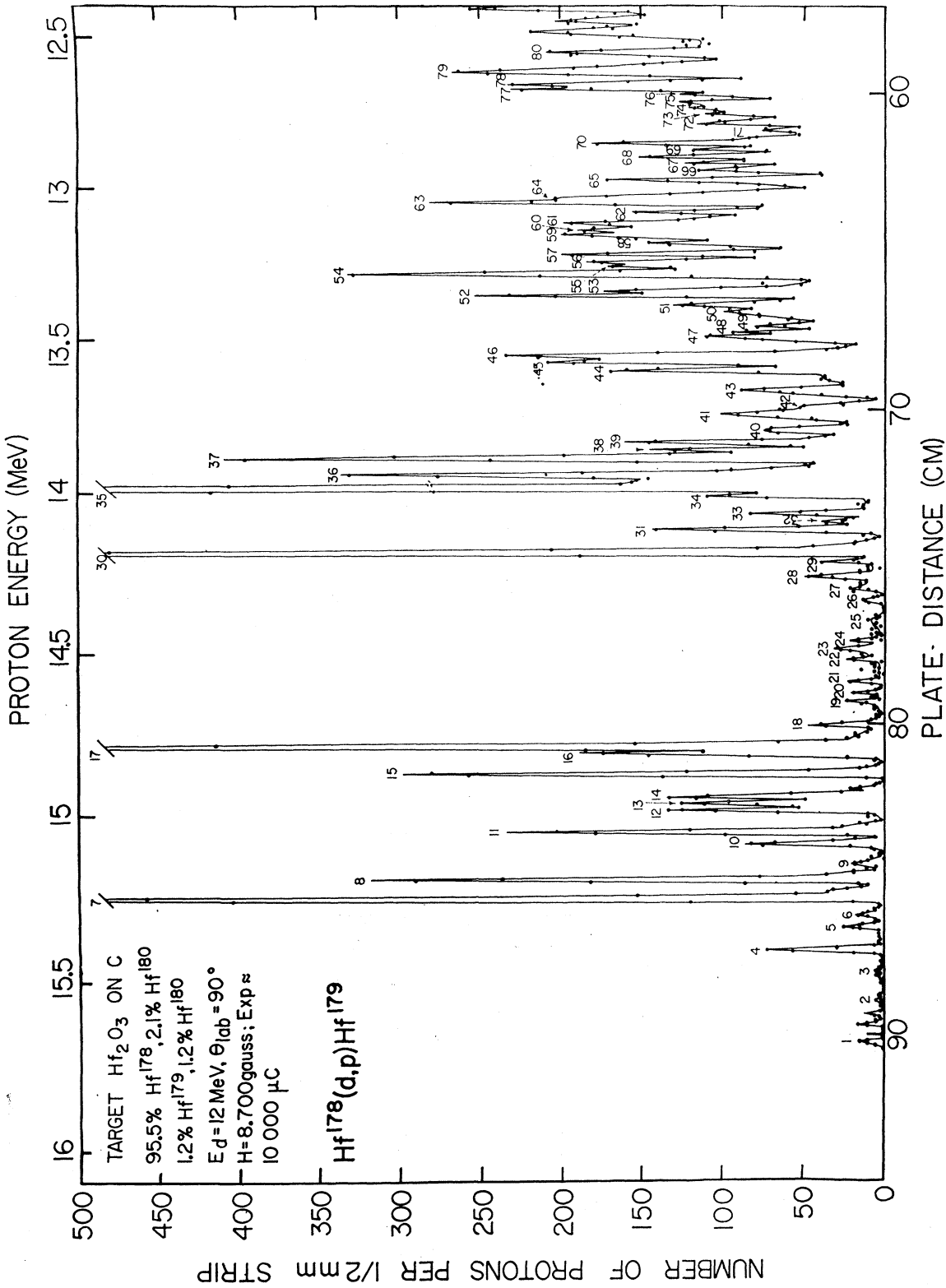
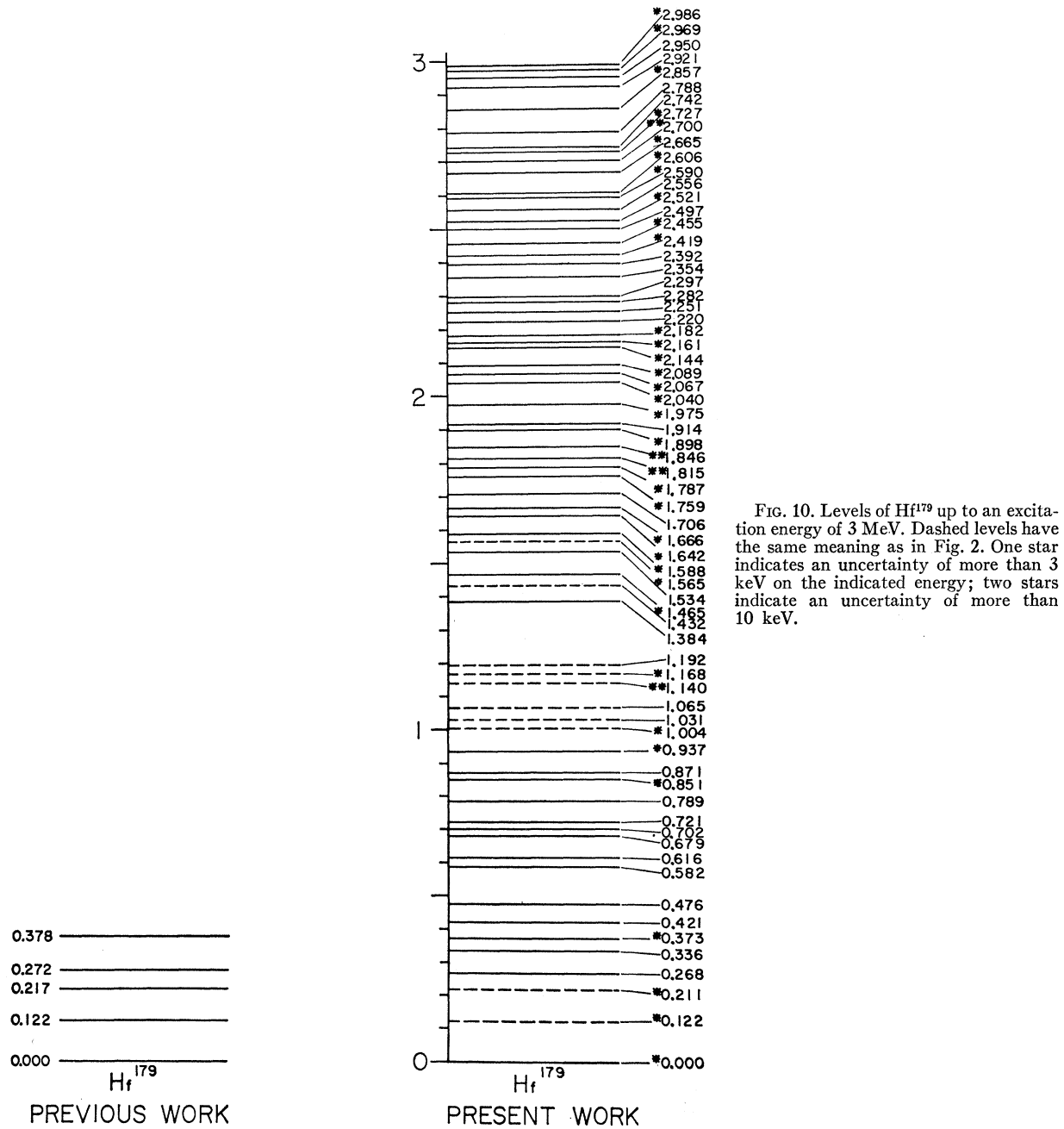


Fig. 9. Typical proton spectrum for the reaction Hf¹⁷⁸(d,p)Hf¹⁷⁹.



factory. Therefore, the 1365-keV level is tentatively assumed to correspond to the $\frac{3}{2}^-(501)$ Nilsson orbital.

Up to an energy of 1.6 MeV, 17 out of 26 levels have been assigned, representing a total theoretical differential cross section at $\theta = 90^\circ$ of 2.214 mb/sr. The total experimental differential cross section up to this energy is 2.27 mb/sr. Some of the nine unassigned levels may correspond to other Yb isotopes or heavy impurities. Most of them are probably members of the rotational bands listed in Table IV as corresponding to small cross sections.

Because of the increase of level density, no exact identification will be attempted above 1.6 MeV. It should be indicated, however, that the total theoretical cross section of 1.44 mb/sr at $\theta = 90^\circ$ corresponding to the two last rotational bands in Table IV is very close to the experimental value of 1.33 mb/sr measured for the group of levels appearing between 1.9 and 2.25 MeV.

The level scheme obtained for Yb^{177} up to an excitation energy of 1.6 MeV is given in Fig. 8. The letters A and B give an indication of the reliability of the results.

TABLE VIII. Relative intensities of the proton peaks for the $\text{Hf}^{178}(d,p)\text{Hf}^{179}$ reaction.^a

Excitation energy (keV)	Number of peak in Fig. 9	25°	35°	45°	55°	65°	77°	90°
268	4	<i>w</i>	<i>w</i>	<i>w</i>	<i>w</i>	55	75	105
421	7	1000	1000	1000	1000	1000	1000	1000
476	8	180	330	290	425	430	470	520
582	10	90	105	105	90	125	130	175
616	11	170	170	160	290	290	280	390
679	12	180	120	160	200	190	205	230
702	13	110	110	135	175	190	165	215
721	14	305	180	140	230	255	205	230
789	15	240	255	260	325	370	355	480
851	16	135	125	160	190	195	290	<330
871	17	370	465	530	675	780	730	1220
937	18	<i>w</i>	<i>w</i>	<i>w</i>	<i>w</i>	60	70	85
1465	30	<860	320	800	1190	990	950	1290
1534	31	<i>a</i>	<i>a</i>	125	200	230	250	265
1588	33	185	105	70	100	100	115	150
1642	34	~170	<75	105	140	~170	140	<190
1666	35	1920	1120	1600	2030	1970	1790	2080
1707	36	370	<i>a</i>	245	375	475	390	550
1759	37	260	<i>a</i>	245	~440	465	460	670
1787	38	~200	<150	~100	<150	150	180	240
1815	39	260	160	135	230	280	185	265
1846	40	~140	130	~60	120	130	95	150
1898	41	~115	<100	~90	100	180	115	165
1914	42	~85	<100	~80	<i>w</i>	<i>a</i>	100	<110
1975	43	~60	70	~80	~90	~115	130	150

^a The entry "a" means that the peak is hidden at this angle by a light impurity peak; "w" indicates a weak peak (≤ 50).

V. $\text{Hf}^{178}(d,p)\text{Hf}^{179}$ REACTION

A typical proton spectrum for the reaction $\text{Hf}^{178}(d,p)\text{Hf}^{179}$ is given in Fig. 9. The possibility of contamination by heavy nuclei during the preparation of the targets is increased in this case because of the very high temperature needed to evaporate the Hf oxide. However, this possible contamination is assumed to be low since few light impurities are present. Because of the very high isotopic enrichment (95.5%), all the levels remaining after elimination of the light impurities are considered to be excited levels of Hf^{179} . These levels, up to an excitation energy of 3 MeV are given in Fig. 10.

Table VIII gives the relative intensities at several angles of most of the proton peaks up to an excitation energy of 2 MeV. The normalization is the same as in Table I, the normalized level $\frac{3}{2}^-, \frac{1}{2}^- (510)$ appearing this time (see following section) at an excitation energy of 421 keV.

The mean experimental *Q* value for the ground state proton peak is $Q = 3877 \pm 14$ keV, which is within error limits of the calculated¹⁹ value $Q = 3836 \pm 170$ keV.

No monitor run was made for this reaction and therefore no real angular distribution is available. However, some indications of the *l* values can be obtained by comparing the relative angular distributions of Table VIII to the relative angular distributions for Yb^{177} in Table I. This assumes the reasonable hypothesis that the angular distribution of the protons corresponding to the level $\frac{3}{2}^-, \frac{1}{2}^- (510)$ is the same in both nuclei:

Level Scheme

The $\frac{3}{2}^+ (624)$ ground state and the two excited states, $\frac{7}{2}^- (514)$ at 217 keV and $\frac{1}{2}^- (510)$ at 378 keV, were previously known.^{21,26} The two first rotational levels of the ground-state band had also been observed^{22,23} at 122 and 272 keV. Up to an excitation energy of 600 keV, every level of Hf^{179} obtained by (*d, p*) reaction can be identified either with one of these previously known levels or, on the basis of its energy, relative intensity and relative angular distribution, with a rotational level previously assigned in Yb^{177} . This part of the level scheme of Hf^{179} is compared to the corresponding part of the level scheme of Yb^{177} and to previously known levels of Hf^{179} in Fig. 11. The decoupling parameter for the $\frac{1}{2}^- (510)$ band in Hf^{179} is found to be $a = +0.165$; the corresponding inertial parameter is $\hbar^2/2\mathcal{I} = 13.22$ keV.

Above 600 keV, the experimental data are not sufficient to permit assignment of angular momenta, parities, or Nilsson orbitals. It will only be remarked that the proton spectrum of Fig. 9 presents at least two striking differences with the proton spectrum of Fig. 1 which corresponds to the reaction $\text{Yb}^{176}(d,p)\text{Yb}^{177}$. The first difference is that the regular sequence of levels assumed to correspond to the rotational band $\frac{3}{2}^- (512)$ in Yb^{177} is no longer evident among the levels of Hf^{179} . It must be concluded that either the sequence observed in Yb^{177} is purely fortuitous and the levels do

²⁶ K. W. Hoffman, I. Y. Krause, W. D. Schmidt-Ott, and A. Flammersfeld, Z. Physik 154, 408 (1959).

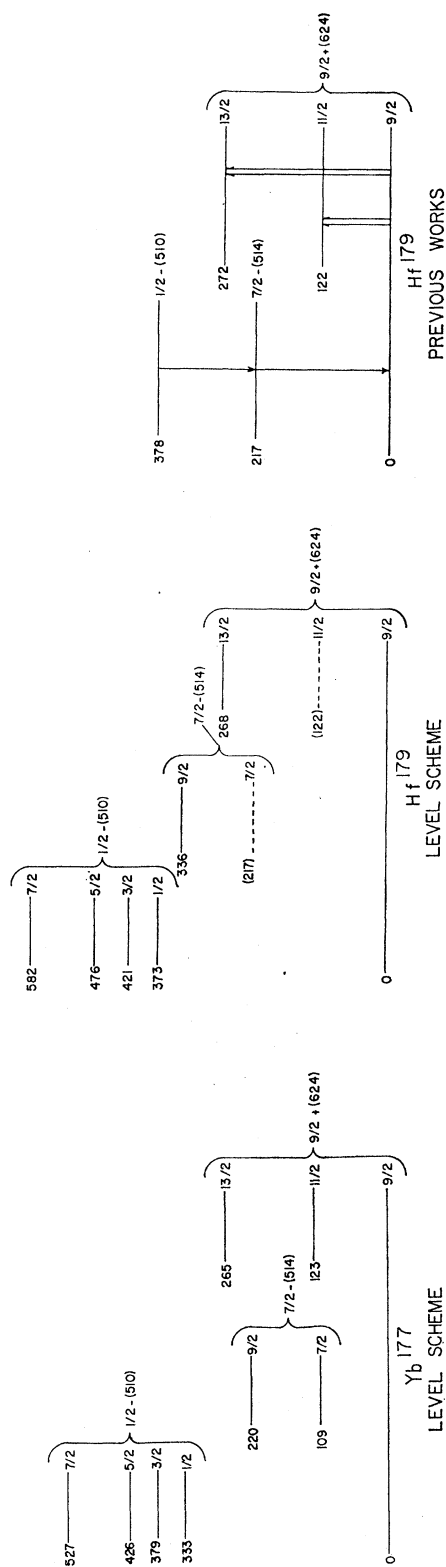


FIG. 11. Comparison of the level schemes obtained from (d,p) reaction data for the lowest levels of Yb^{177} and Hf^{179} . The previously known levels of Hf^{179} are also indicated.

not correspond to the $\frac{3}{2}^-$ (512) rotational band, or the relative intensities of the members of this band are deeply modified in Hf^{179} . The second difference is that, in strong contrast with the proton spectrum of Fig. 1, the proton spectrum for the reaction $Hf^{178}(d,p)Hf^{179}$ presented in Fig. 9 does not exhibit any very big peaks between excitation energies of 1.7 and 3 MeV. Although no explanation can be advanced, it can be remarked that in a previous work²⁷ on the $E1$ transition probabilities, an anomalous behavior has also been observed for the nucleus Hf^{179} as compared to neighboring deformed nuclei.

VI. COMPARISON OF THE LOWEST EXCITED STATES OF THE 107-NEUTRON ISOTONES

It seems well established that the ground states of all the 107-neutron nuclei correspond to the $\frac{9}{2}^+$ (624) Nilsson orbital. The first intrinsic excited level corresponds to the $\frac{7}{2}^-$ (514) orbital and appears at 104 keV in Yb^{177} , 217 keV in Hf^{179} , and probably²⁸ 409 keV in W^{181} , moving upward in energy quite regularly from isotone to isotone as the mass number increases. The second intrinsic excited level corresponds to the $\frac{1}{2}^-$ (510) orbital and appears at 333 keV in Yb^{177} , 373 keV in Hf^{179} , and 171 keV in Os^{188} . Its position is not clearly established among the excited levels of W^{181} . It appears at 515 keV in the decay scheme given by Mottelson and Nilsson²⁹ and at 385 keV in the decay scheme of Harmatz, Handley, and Mihelich.²⁸

The value of the decoupling parameter of the $\frac{1}{2}^-$ (510) rotational band has been found to be $a = +0.22$ in Yb^{177} and $a = +0.165$ in Hf^{179} . Its value was known²⁹ to be $a = +0.19$ in the 109-neutron nucleus W^{188} . These three values are very close and are quite different from the value of $a = +0.48$ found by H.H.M.²⁸ for W^{181} . The value of $a = +0.165$ obtained with the decay scheme of M.N.²⁹ seems more satisfactory.

An attempt has been made by Solov'ev²⁵ to compute the positions of the first quasiparticle levels in a 107-neutron nucleus. The Nilsson orbitals are used as single-particle levels and the computations are performed for several values of G , the strength of the pairing force. For any value of G the $\frac{9}{2}^+$ (624) orbital is found to be the ground state and the $\frac{7}{2}^-$ (514) orbital to be the first excited state. For a value of $G = 0.16$ MeV, the two first excited states $\frac{7}{2}^-$ (514) and $\frac{1}{2}^-$ (510) are predicted to appear, respectively, at 118- and 330-keV above the $\frac{9}{2}^+$ (624) ground state. These values are amazingly close to the experimental values found in Yb^{177} : 104 keV for the $\frac{7}{2}^-$ (514) orbital and 333 keV for the $\frac{1}{2}^-$ (510) orbital. Unfortunately, the model is not so good for the next two intrinsic excited states, $\frac{3}{2}^-$ (512) and $\frac{7}{2}^-$ (503); for the same value of G they

²⁷ M. N. Vergnes, J. Phys. Radium **24**, 131 (1963).

²⁸ B. Harmatz, T. H. Handley, and J. W. Mihelich, Phys. Rev. **119**, 1345 (1960).

²⁹ B. R. Mottelson and S. G. Nilsson, Kgl. Danske Videnskab. Selskab, Mat. Fys. Skrifter **1**, 8 (1959).

are predicted to appear at 380 and 430 keV, when the probable values found in Yb¹⁷⁷ are 709 and 1226 keV.

VII. CONCLUSIONS

Many previously unknown excited levels of Yb¹⁷⁷ and Hf¹⁷⁹ have been identified and studied in this work. When it was possible they were assigned with varying degrees of certainty to intrinsic Nilsson orbitals or their associated rotational bands.

It has been shown that (*d, p*) reactions on deformed even-even target nuclei can be well explained theoretically using the DWBA theory of Tobocman to compute the intrinsic single-particle cross section, the Satchler theory to compute the spectroscopic factor, and the Nilsson wave functions to describe the intrinsic excitations.

It can be concluded that the stripping reactions, which have been proved to be a very valuable spectroscopic tool for spherical nuclei, can also be used successfully for the study of deformed nuclei. The detailed analysis of the results even suggests that it should be possible to obtain in this way direct information about the wave functions themselves.

ACKNOWLEDGMENTS

The authors wish to thank C. L. Nealy and G. L. Struble for their invaluable assistance in running the accelerator and taking data, A. Sperduto for a very helpful discussion, Dr. G. R. Satchler for providing the DWBA computations, and the plate scanners for their careful work.

One of us (M.N.V.) wishes to thank the NATO for the grant of a post-doctoral fellowship.

APPENDIX

Tables of the coefficients $C_{j,l}$ and $C^2_{j,l}$ for the neutron Nilsson levels⁸ of interest in the rare-earth deformed odd-*A* nuclei. The computations were performed for two values of the deformation parameter: $\delta=0.2$ and $\delta=0.3$.

Level $\frac{1}{2}-[541]$.

		$\delta \backslash \begin{matrix} j,l \\ \hline \end{matrix}$	11/2, 5	9/2, 5	7/2, 3	5/2, 3	3/2, 1	1/2, 1
<i>C</i>	0.2		-0.3067	-0.5171	0.4386	-0.4433	0.4211	-0.2686
	0.3		-0.3826	-0.5272	0.2013	-0.5364	0.3725	-0.3296
<i>C</i> ²	0.2		0.0941	0.2674	0.1924	0.1965	0.1774	0.0722
	0.3		0.1464	0.2779	0.0405	0.2877	0.1388	0.1086

Level $\frac{1}{2}-[530]$.

		$\delta \backslash \begin{matrix} j,l \\ \hline \end{matrix}$	11/2, 5	9/2, 5	7/2, 3	5/2, 3	3/2, 1	1/2, 1
<i>C</i>	0.2		0.2559	-0.6636	-0.5394	-0.2797	-0.3532	0.0120
	0.3		0.3808	-0.5880	-0.4813	-0.2421	-0.4612	0.0779
<i>C</i> ²	0.2		0.0655	0.4404	0.2910	0.0782	0.1247	0.0001
	0.3		0.1450	0.3458	0.2317	0.0586	0.2127	0.0061

Level $\frac{3}{2}-[532]$.

		$\delta \backslash \begin{matrix} j,l \\ \hline \end{matrix}$	11/2, 5	9/2, 5	7/2, 3	5/2, 3	3/2, 1
<i>C</i>	0.2		-0.2580	-0.7375	0.4368	-0.3958	0.2050
	0.3		-0.3222	-0.7516	0.2853	-0.4600	0.1956
<i>C</i> ²	0.2		0.0666	0.5439	0.1908	0.1566	0.0420
	0.3		0.1038	0.5648	0.0814	0.2117	0.0382

Level $\frac{1}{2}+[660]$.

		$\delta \backslash \begin{matrix} j,l \\ \hline \end{matrix}$	13/2, 6	11/2, 6	9/2, 4	7/2, 4	5/2, 2	3/2, 2	1/2, 0
<i>C</i>	0.2		0.9142	-0.0215	0.3845	-0.0184	0.1205	-0.016	-0.028
	0.3		0.8204	-0.0416	0.5103	-0.0506	0.2323	-0.0513	0.0756
<i>C</i> ²	0.2		0.8357	0.0004	0.1478	0.0003	0.0145	0.0002	0.0008
	0.3		0.6731	0.0017	0.2604	0.0026	0.0539	0.0026	0.0057

Level $\frac{3}{2}^+$ [651].

	$\delta \backslash j, l$	13/2, 6	11/2, 6	9/2, 4	7/2, 4	5/2, 2	3/2, 2
C	0.2	0.93225	-0.0549	0.3462	-0.0338	0.0818	0.0078
	0.3	0.8694	-0.0894	0.4567	-0.0717	0.1461	-0.0310
C ²	0.2	0.8691	0.0030	0.1199	0.0011	0.0067	~ 0
	0.3	0.7559	0.0080	0.2086	0.0051	0.0213	0.0009

Level $\frac{3}{2}^-$ (521).

	$\delta \backslash j, l$	11/2, 5	9/2, 5	7/2, 3	5/2, 3	3/2, 1
C	0.2	0.2399	-0.5683	-0.7419	-0.0502	-0.2579
	0.3	0.3349	-0.5045	-0.7271	0.0010	-0.3234
C ²	0.2	0.0575	0.3229	0.5505	0.0025	0.0665
	0.3	0.1121	0.2545	0.5287	~ 0	0.1046

Level $\frac{5}{2}^+$ [642].

	$\delta \backslash j, l$	13/2, 6	11/2, 6	9/2, 4	7/2, 4	5/2, 2
C	0.2	0.9549	-0.0756	0.2828	-0.0317	0.0385
	0.3	0.9180	-0.1147	0.3694	-0.0586	0.0645
C ²	0.2	0.9118	0.0057	0.0800	0.0010	0.0015
	0.3	0.8427	0.0132	0.1364	0.0034	0.0042

Level $\frac{5}{2}^-$ [523].

	$\delta \backslash j, l$	11/2, 5	9/2, 5	7/2, 3	5/2, 3
C	0.2	-0.1907	-0.8782	0.3655	-0.2403
	0.3	-0.2463	-0.8882	0.2762	-0.2723
C ²	0.2	0.0364	0.7713	0.1336	0.0577
	0.3	0.0607	0.7889	0.0763	0.0742

Level $\frac{1}{2}^-$ [521].

	$\delta \backslash j, l$	11/2, 5	9/2, 5	7/2, 3	5/2, 3	3/2, 1	1/2, 1
C	0.2	-0.1367	-0.4569	0.4435	0.486	-0.2864	0.508
	0.3	-0.2124	-0.5183	0.4810	0.4265	-0.1563	0.4987
C ²	0.2	0.019	0.209	0.197	0.236	0.082	0.258
	0.3	0.045	0.269	0.2314	0.182	0.0244	0.249

Level $\frac{7}{2}^+$ [633].

	$\delta \backslash j, l$	13/2, 6	11/2, 6	9/2, 4	7/2, 4
C	0.2	0.9755	-0.084	0.204	-0.019
	0.3	0.957	-0.1224	0.2643	-0.0323
C ²	0.2	0.953	0.007	0.04	0.0004
	0.3	0.915	0.015	0.07	0.001

Level $\frac{5}{2}^-$ [512].

	$\delta \backslash j, l$	11/2, 5	9/2, 5	7/2, 3	5/2, 3
C	0.2	0.188	-0.4252	-0.8825	0.063
	0.3	0.25	-0.376	-0.8867	0.1
C ²	0.2	0.035	0.181	0.78	0.004
	0.3	0.0625	0.1413	0.7862	0.01

Level $\frac{7}{2}^-$ [503].

	$\delta \backslash j, l$	11/2, 5	9/2, 5	7/2, 3
C	0.2	0.1137	-0.266	-0.9572
	0.3	0.1468	-0.2321	-0.9615
C ²	0.2	0.013	0.0707	0.916
	0.3	0.0215	0.0539	0.9245

Level $\frac{9}{2}^-$ [505].

	$\delta \backslash j, l$	11/2, 5	9/2, 5
C	0.2	-0.08	0.997
	0.3	-0.106	0.995
C ²	0.2	0.006	0.994
	0.3	0.01	0.99

Level 11/2+ [615].

	$\delta \backslash j, l$	13/2, 6	11/2, 6
C	0.2	0.9979	-0.645
	0.3	0.9962	-0.0874
C ²	0.2	0.9958	0.0042
	0.3	0.9925	0.0076

Level 13/2+ [606].

	$\delta \backslash j, l$	13/2, 6
C	0.2	1.0
	0.3	1.0
C ²	0.2	1.0
	0.3	1.0

Level $\frac{7}{2}^-$ [514].

	$\delta \backslash j, l$	11/2, 5	9/2, 5	7/2, 3
C	0.2	-0.1339	-0.9592	0.2505
	0.3	-0.1745	-0.9629	0.2057
C ²	0.2	0.0179	0.92	0.0627
	0.3	0.03	0.927	0.0423

Level $\frac{3}{2}+[624]$.

	$\delta \begin{smallmatrix} j, l \\ \diagdown \end{smallmatrix}$	13/2, 6	11/2, 6	9/2, 4
C	0.2	0.9897	-0.0818	0.1187
	0.3	0.982	-0.1137	0.1507
C ²	0.2	0.98	0.006	0.014
	0.3	0.964	0.0129	0.0227

Level $\frac{1}{2}-[510]$.

	$\delta \begin{smallmatrix} j, l \\ \diagdown \end{smallmatrix}$	11/2, 5	9/2, 5	7/2, 3	5/2, 3	3/2, 1	1/2, 1
C	0.2	0.0794	-0.2684	-0.3713	0.5686	0.6755	-0.058
	0.3	0.1227	-0.2962	-0.4362	0.5406	0.6358	-0.0967
C ²	0.2	0.0063	0.072	0.138	0.323	0.456	0.0034
	0.3	0.015	0.088	0.19	0.292	0.405	0.01

Level $\frac{3}{2}-[512]$.

	$\delta \begin{smallmatrix} j, l \\ \diagdown \end{smallmatrix}$	11/2, 5	9/2, 5	7/2, 3	5/2, 3	3/2, 1
C	0.2	-0.0715	-0.3369	0.2963	0.8245	-0.338
	0.3	-0.11	-0.3857	0.3442	0.8	-0.282
C ²	0.2	0.0051	0.1135	0.0880	0.680	0.1140
	0.3	0.012	0.149	0.118	0.64	0.08

Level $\frac{3}{2}-[501]$.

	$\delta \begin{smallmatrix} j, l \\ \diagdown \end{smallmatrix}$	11/2, 5	9/2, 5	7/2, 3	5/2, 3	3/2, 1
C	0.2	0.04	-0.1184	-0.231	0.398	0.88
	0.3	0.05	-0.128	-0.275	0.373	0.875
C ²	0.2	0.0016	0.014	0.0533	0.1583	0.7744
	0.3	0.0025	0.0164	0.076	0.14	0.765

Level $\frac{3}{2}-[503]$.

	$\delta \begin{smallmatrix} j, l \\ \diagdown \end{smallmatrix}$	11/2, 5	9/2, 5	7/2, 3	5/2, 3
C	0.2	-0.03	-0.1938	0.1553	0.9684
	0.3	-0.045	-0.2215	0.19	0.9555
C ²	0.2	0.001	0.0375	0.0241	0.9377
	0.3	0.002	0.049	0.036	0.913

Level $\frac{1}{2}-[501]$.

	$\delta \begin{smallmatrix} j, l \\ \diagdown \end{smallmatrix}$	11/2, 5	9/2, 5	7/2, 3	5/2, 3	3/2, 1	1/2, 1
C	0.2	-0.0217	-0.104	0.1345	0.405	-0.3761	-0.8146
	0.3	-0.036	-0.1234	0.1716	0.4114	-0.403	-0.787
C ²	0.2	0.0004	0.0109	0.0181	0.1643	0.1417	0.6632
	0.3	0.0013	0.0152	0.0295	0.1718	0.1623	0.619